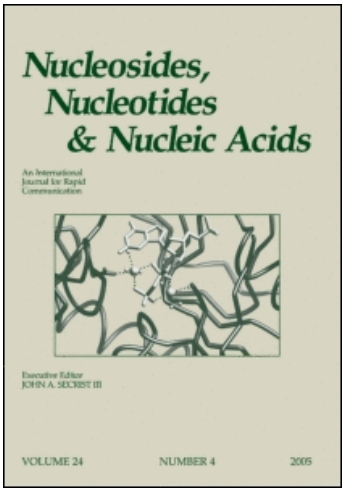

Nucleosides, Nucleotides and Nucleic Acids
Publication details, including instructions for authors and subscription information:
http://www.informaworld.com/smpp/title~content=t713597286

STRUCTURAL, DYNAMIC, AND ENZYMATIC PROPERTIES OF MIXED α/β-OLIGONUCLEOTIDES CONTAINING POLARITY REVERSALS

M. W. Germann[a]; J. M. Aramini[a]; B. W. Kalisch[b]; J. H. van de Sande[b]
[a] Department of Microbiology and Immunology, Kimmel Cancer Institute, Thomas Jefferson University, Philadelphia [b] Department of Medical Biochemistry, University of Calgary, Calgary, Canada

Online publication date: 31 March 2001

To cite this Article Germann, M. W. , Aramini, J. M. , Kalisch, B. W. and van de Sande, J. H.(2001) 'STRUCTURAL, DYNAMIC, AND ENZYMATIC PROPERTIES OF MIXED α/β-OLIGONUCLEOTIDES CONTAINING POLARITY REVERSALS', Nucleosides, Nucleotides and Nucleic Acids, 20: 4, 493 — 499
To link to this Article: DOI: 10.1081/NCN-100002324
URL: http://dx.doi.org/10.1081/NCN-100002324

NUCLEOSIDES, NUCLEOTIDES & NUCLEIC ACIDS, 20(4–7), 493–499 (2001)

STRUCTURAL, DYNAMIC, AND ENZYMATIC PROPERTIES OF MIXED α/β-OLIGONUCLEOTIDES CONTAINING POLARITY REVERSALS

M. W. Germann,[1,*] J. M. Aramini,[1] B. W. Kalisch,[2] and J. H. van de Sande[2]

[1]Department of Microbiology and Immunology, Kimmel Cancer Institute, Thomas Jefferson University, Philadelphia 19107
[2]Department of Medical Biochemistry, University of Calgary, Calgary, Alberta, Canada T2N 4N1

ABSTRACT

We employ NMR structure determination, thermodynamics, and enzymatics to uncover the structural, thermodynamic and enzymatic properties of α/β-ODNs containing 3′-3′ and 5′-5′ linkages. RNase H studies show that α/β-gapmers that are designed to target *erb*B-2 efficiently elicit RNase H activity. NMR structures of DNA · DNA and DNA · RNA duplexes reveal that single α-anomeric residues fit well into either duplex, but alter the dynamic properties of the backbone and deoxyriboses as well as the topology of the minor groove in the DNA · RNA hybrid.

INTRODUCTION

Interest in antisense ODN therapy has generated a flurry of modifications to bases, sugars and backbones in order to enhance the potential therapeutic properties of ODNs designed to inhibit gene expression at a translational (mRNA) level (1). Desirable properties of potential antisense ODNs include: high nuclease resistance, high affinity and selectivity towards the intended target mRNA, cellular uptake, synthetic feasibility and RNase H cleavage of the mRNA in complex with the

*Corresponding author.

ODN. However, with very few exceptions, most modifications result in ODNs that ablate RNase H action. This has led to the design of chimeric ODNs containing nuclease resistant components and segments that elicit RNase H activity (2).

Research on alpha-anomeric ODNs as potential antisense agents established their ability to form stable hybrids with complementary β-DNA and β-RNA sequences (3), resistance to nuclease degradation (4), and inhibition of mRNA translation and viral growth in an RNase H-independent manner (5). Moreover, chimeric α/β-ODNs, featuring phosphodiester linkage reversals (6,7) have been shown to support RNase H mediated mRNA destruction *in vitro* (8,9). Recently, such constructs were reported to selectively inhibit growth in two cervical carcinoma cell lines as well as in tumor bearing mice (10).

In this paper we present a summary of our current knowledge of the properties of chimeric α/β-ODNs containing 3′-3′ and 5′-5′ polarity reversals with particular emphasis on their RNase H activation and structural/dynamic features.

RNase H STUDIES

Among the many characteristic factors in breast cancer the oncogene c-*erb*B-2 is amplified and overexpressed in over 30% of early and advanced mammary tumors (as well as in ovarian malignancies) where it coincides with poor prognosis (11,12). The α/β-ODNs containing polarity reversals that we are using in our proof-of-principle studies target *erb*B-2 mRNA (Fig. 1). This target has been tested with six different overlapping antisense sequences, and several control sequences and cancer cell lines (13,14). Sequences Alpha3-7 address the importance of the size of the β-anomeric window for RNAse H activity. The design of these sequences enables the parallel stranded orientation of the α-anomeric wings with respect to

5′-dCTCCATGGTGCTCAC	DNA
5′-dCTCCATGGTGCTCAC	PS
3′-d***CTCCATGGTGCTCAC***	alpha
3′-d***CTCCAT***-5′5′-GGT-3′3′-***GCTCAC***	Alpha3
3′-d**CTCCA**-5′5′-TGGT-3′3′-***GCTCAC***	Alpha4
3′-d**CTCCA**-5′5′-TGGTG-3′3′-***CTCAC***	Alpha5
3′-d***CTCC***-5′5′-ATGGTG-3′3′-***CTCAC***	Alpha6
3′-d***CTCC***-5′5′-ATGGTGC-3′3′-***TCAC***	Alpha7
5′-d*CTCCA*TGGT*GCTCAC*	2′-Ome4
5′-d*CTCCA*TGGTG*CTCAC*	2′-Ome5
***erb*B-2 mRNA** 5′-rGCCGCAGUGAGCACCAUGGAGCUGGCGGCC…3′	

Figure 1. 15mer ODN sequences targeting *erb*B-2 mRNA. Natural β-anomeric nucleotides are underlined, α-anomeric nucleotides are bold and italics, and 2′-O Methyl containing nucleotides are in italics only. ***erb*B-2 mRNA:** RNA target; the 15-mer used in the RNase H reactions is shown in larger lettering.

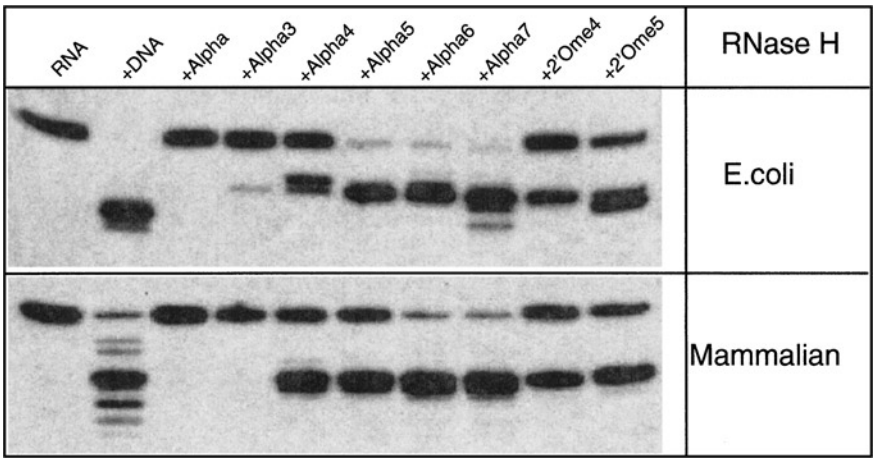

Figure 2. Denaturing gel electrophoretic analysis of *E. coli* and Mammalian RNase H substrate properties. Reactions contain 0.3 OD/ml ^{32}P labeled RNA and 0.87 unit RNase H (*E. coli*, Pharmacia, or 1 μl rabbit reticulocyte lysate, Promega). The ODN concentration was 0.6 OD/ml. Reactions were run at 37°C for 30 minutes, terminated with formamide and applied to a 20% denaturing polyacrylamide gel.

the RNA target. In order to compare the efficacy of the α/β-gapmer ODNs, control sequences comprised of all α-anomeric nucleotides (alpha), all phosphorothioate backbone (PS), and gapmers featuring 4 or 5 β-anomeric residues flanked by 2′-O-methyl stretches (2′-Ome4 and 2′-Ome5) were also studied.

RNase H substrate properties of the ODN · RNA hybrids were determined for mammalian RNase H as well as for *E. coli* RNase H (Fig. 2). It is readily apparent that a β-anomeric window of three nucleotides is sufficient to allow limited *E. coli* RNase H activity. This is remarkable, since this window only contains two natural phosphodiester linkages. As expected, increasing the window size improves the substrate quality of the ODN as measured from the digestion of the ^{32}P labeled 15mer RNA (control 94%, alpha 0%, Alpha3 3%, Alpha4 30%, Alpha5 80%, Alpha6 87%, Alpha7 93%, 2′-Ome4 21%, 2′-Ome5 42%). It is evident that the α-winged ODNs are better substrates than the corresponding 2′-O-Me sequences. The preferred cutting site is across the 5′-5′ linkage of the ODN (on the 3′ side of the RNA with respect to the window).

For mammalian RNase H a four β-anomeric window (three natural phosphodiester linkages) is sufficient (control 87%, alpha 0%, Alpha3 0%, Alpha4 66%, Alpha5 70%, Alpha6 85%, Alpha7 88%, 2′-OMe4 53%, 2′-OMe5 67%). Again we observe that the α-winged oligonucleotides outperform the 2′-O-Me sequences. The preferred site of RNA hydrolysis for the mammalian enzyme is at the center of the β-anomeric window in contrast to what was observed for *E. coli* RNase H. All gapmer constructs performed considerably better than the PS ODN for which 49% of the RNA was hydrolyzed.

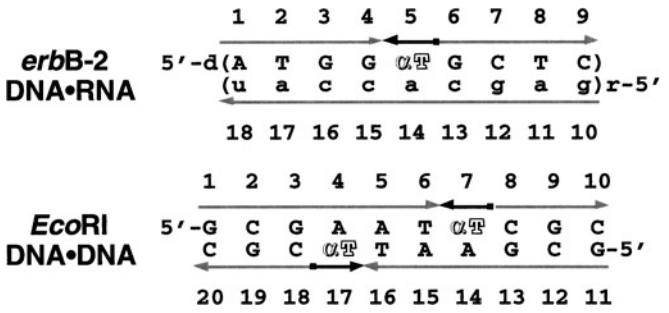

Figure 3. Sequences of the self-complementary *Eco*RI DNA · DNA decamer duplex and *erb*B-2 DNA · RNA nonamer hybrid. Arrows indicate the strand polarity in the 5′ → 3′ direction, with the unusual phosphodiester linkages in the DNA strands denoted by head-to-head (3′-3′) and tail-to-tail (5′-5′) junctions.

NMR STRUCTURES

The previous section demonstrates the need for understanding the structural details of α-anomeric residues combined with linkage reversals. We have therefore determined the NMR structures of DNA · DNA and DNA · RNA systems containing single α-anomeric residues inserted with 3′-3′ and 5′-5′ linkages (Fig. 3) (15,16). The DNA · DNA self-complementary decamer duplex features a central *Eco*RI restriction enzyme site, while the DNA · RNA nonamer hybrid corresponds to the core of the *erb*B-2 target discussed above. In both cases, thermodynamic and spectroscopic (UV and CD) studies established that the 3′-3′-αT-5′-5′ modification results in a surprisingly small decrease in thermostability and little change in global structure compared to unmodified controls (16,17).

Using NOE-based MARDIGRAS-derived distance restraints and *J*-based deoxyribose ring torsion angle restraints, *in vacuo* structures of *Eco*RI DNA · DNA and *erb*B-2 DNA · RNA were determined by conventional restrained molecular dynamics, rMD (Fig. 4A.)* (15,16). The DNA duplex adopts an overall right-handed B-type structure, highly superimposable with that of the unmodified control decamer duplex, featuring normal Watson-Crick base pairing and stacking throughout. However, a number of local structural perturbations are evident within each region encompassing the modifications, including increased pseudorotation phase angle, *P*, of the α-nucleotide, altered sugar ring conformation in the nucleotide following the 5′-5′ linkage, and unusual backbone torsion angles in both the 3′-3′ and 5′-5′ linkages. In the case of the hybrid, the polarity reversed αT fits snugly into an overall A-like duplex that nonetheless exhibits local B-like traits, namely S-type puckering from T2 to αT5 and a concomitant decreased minor groove width upstream of the 3′-3′ junction. Other sugar and backbone perturbations analogous to those in the DNA duplex were also observed.

* Please see color insert for Figure 4.

The final *in vacuo* structures are static models, after all, and do not reflect the inherent dynamics of these molecules, in particular sugar repuckering events and backbone mobility; this issue is addressed in the next section.

CONFORMATIONAL DYNAMICS

A more comprehensive description of the conformational dynamics of the DNA decamer duplex and DNA · RNA hybrid was achieved using molecular dynamics with time-averaged NMR restraints, MDtar (19,20). In this approach experimental restraints are required to be satisfied over a period of time within an rMD run on a single copy of the molecule of interest. In contrast to conventional rMD in which restraints are enforced at each point in the trajectory resulting in potentially unrealistic average structures, MDtar facilitates wider excursions in conformational space. MDtar and multiple-copy refinement approaches (21) have emerged as successful methods for describing the conformational dynamics in nucleic acids predicted by NMR.

MDtar calculations were performed starting from the final *in vacuo* rMD structures in the presence of explicit water and counterions (18). Only the NOE-based distance restraints were applied in a time-averaged fashion; no *J*-based deoxyribose ring torsion angle restraints were used in the MDtar calculations. For both duplexes, we found much better agreement with the experimental NOE *and J*-data, reflected by average distance and coupling constant violations and improved sixth-root *R*-factors. The deoxyribose ring puckering behavior throughout both molecules agrees remarkably well with that predicted by pseudoroation theory (22) on the basis of the *J*-coupling constant values (represented in Fig. 4A). This is especially gratifying for the DNA · RNA hybrid, in which the DNA strand exhibits the entire range of puckering behavior, from high fraction of S- to high fraction of N-puckering; this is exemplified in Figure 5, which compares the rMD and MDtar trajectories of G4, αT5, and G6. Notice that this procedure does not introduce conformational flexibility where it is not warranted. Also dynamic sugars, such as G6, exhibit a bimodal distribution of N- and S-puckering modes with little occupancy of the intermediate O4′-*endo* state which is an artifact in the more restrictive rMD calculations.

In the region encompassing the α-anomeric nucleotides and polarity reversals, the predicted dynamics were confirmed: 1) backbone torsion angles constitituting the 3′-3′ linkage are relatively static, as well as the deoxyribose rings of the α-thymidine and preceding nucleotides in the sequence; 2) the conformations of the backbone comprising 5′-5′ linkage and the sugar are highly labile. This is reflected in Figure 4B above, where the large number of structures obtained from the MDtar trajectories were distilled to representative ensembles using the PDQPRO program (23).

CONCLUSIONS

The biological potential of α/β-ODNs containing polarity reversals, together with their synthetic feasibility and features that are readily amenable for optimization, make relevant the need for gaining an in-depth understanding of the factors

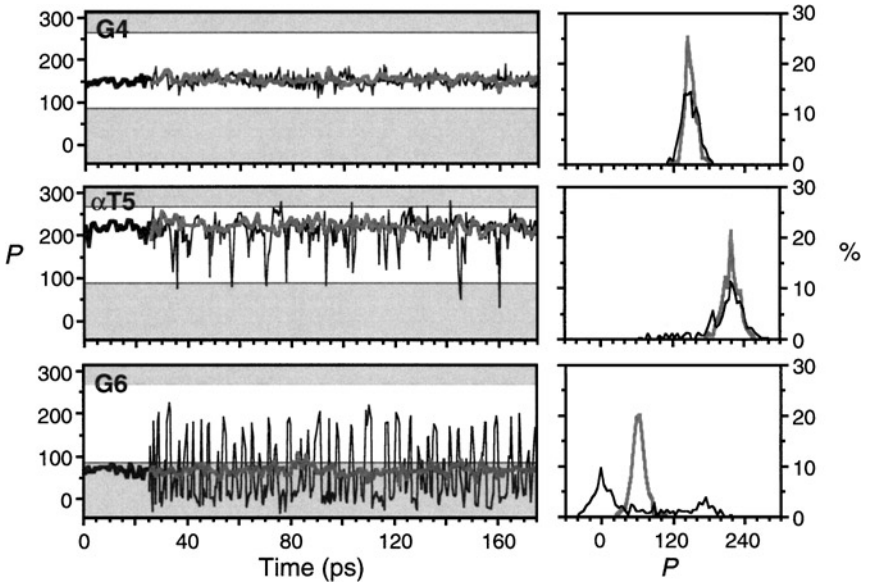

Figure 5. Time courses and relative populations of the pseudorotation phase angle (*P*) for selected deoxyribonucleotides from 150 ps rMD (thick lines) and MDtar (black lines) calculations on *erb*B-2 DNA · RNA in water, following a 25 ps rMD equilibration (AMBER 4.1) (18). Values of *P* corresponding to the N-hemisphere of the pseudorotation wheel are shaded. Relative percentages of *P* represent 5° windows from 0° to 360°.

governing their stability, specificity and RNase H activity. Our RNase H enzymatic studies on the *erb*B-2 system have established the efficacy of α/β-ODNs compared to other modifications, as well as the minimum β-anomeric gap requirements for the *E. coli* and mammalian enzymes. Structurally, in the case of both DNA · DNA and DNA · RNA duplexes the 5′-5′ linkage introduces a dynamic hotspot, evident from the behavior of both the sugar puckering and backbone. The 3′-3′ linkage is static and in the case of the DNA duplex no apparent effect on the sugar puckering is observed. This is in contrast to the DNA · RNA hybrid in which this linkage, albeit static as well, shifts two β-anomeric sugars upstream of the 3′-3′ linkage to essentially purely S-puckering. Together with the α-anomeric residue the modifications result in a stretch of high S-sugars on the DNA strand of the hybrid with an accompanied reduction in minor groove width. Thus, these observations demonstrate that such modifications enable us to locally control the sugar puckering and the topology of the minor groove.

REFERENCES

1. For recent reviews, see: Baker, B. F.; Monia, B. P. *Biochim. Biophys. Acta*, **1999**, *1489*, 3–18; Crooke, S. T. *Methods Enzymol.*, **2000**, *313*, 3–45.

MARCEL DEKKER, INC.
270 Madison Avenue, New York, New York 10016

2. See for example: Monia, B. P.; Lesnik, E. A.; Gonzalez, C.; Lima, W. F.; McGee, D.; Guinosso, C. J.; Kawasaki., A. M.; Cook, P. D.; Freier, S. M. *J. Biol. Chem.*, **1993**, *268*, 14514–14522; Larrouy, B.; Boiziau, C.; Sproat, B.; Toulmé, J.-J. *Nucleic Acids Res.*, **1995**, *23*, 3434–3440; Agrawal, S.; Jiang, Z.; Zhao, Q.; Shaw, D.; Cai, Q.; Roskey, A.; Channavajjala, L.; Saxinger, C.; Zhang, R. *Proc. Natl. Acad. Sci. USA*, **1997**, *94*, 2620–2625.
3. See for example: Paoletti, J.; Bazile, D.; Morvan, F.; Imbach, J.-L.; Paoletti, C. *Nucleic Acids Res.*, **1989**, *17*, 2693–2704.
4. Vichier-Guerre, S.; Pompon, A.; Lefebvre, I; Imbach, J.-L. *Antisense Res. Dev.*, **1994**, *4*, 9–18.
5. See for example: Bertrand J.-R.; Imbach J.-L.; Paoletti C.; Malvy C. *Biochem. Biophys. Res. Commun.*, **1989**, *164*, 311–318; Lavignon, M.; Tounekti, N.; Rayner, B.; Imbach, J.-L.; Keith, G.; Paoletti, J.; Malvy, C. *Antisense Res. Dev.*, **1992**, *2*, 315–324.
6. Debart, F.; Tosquellas, G.; Rayner, B.; Imbach, J.-L. *Bioorg. Med. Chem. Lett.*, **1994**, *4*, 1041–1046.
7. Koga, M.; Wilk, A.; Moore, M. F.; Scremin, C. L.; Zhou, L.; Beaucage, S. L. *J. Org. Chem.*, **1995**, *60*, 1520–1530.
8. Boiziau, C.; Debart, F.; Rayner, B.; Imbach, J.-L.; Toulmé, J.-J. *FEBS Lett.*, **1995**, *361*, 41–45.
9. Aramini, J. M., van de Sande, J. H.; Germann, M. W. In ACS *Symposium Series 682: Molecular Modeling of Nucleic Acids* (Eds., Leontis, N. B. and SantaLucia Jr., J.), American Chemical Society, Washington, D.C., **1998**, pp. 92–105.
10. Tan, T. M. C.; Kalisch, B. W.; van de Sande, J. H.; Ting, R. C. Y.; Tan, Y. H. *Antisense Nucleic Acid Drug Dev.*, **1998**, *8*, 95–101.
11. Slamon, D. J.; Clark, G. M.; Wong, S. G.; Levin, W. J.; Ullrich, A.; McGuire, W. L. *Science*, **1987**, *235*, 177–182.
12. Slamon, D. J.; Godolphin, W.; Jones, L. A.; Holt, J. A.; Wong, S. G.; Keith, D. E.; Levin, W. J.; Stuart, S. G.; Udove, J.; Ullrich, A.; Press, M. F. *Science*, **1989**, *244*, 707–712.
13. Brysch, W.; Magal, E.; Louis, J.-C.; Kunst, M.; Klinger, I.; Schlingensiepen, R.; Schlingensiepen, K.-H. *Cancer Gene Ther.*, **1994**, *1*, 99–105.
14. Vaughn, J. P.; Iglehart, J. D.; Demirdji, S.; Davis, P.; Babiss, L. E.; Caruthers, M. H.; Marks, J. R. *Proc. Natl. Acad. Sci USA*, **1995**, *92*, 8338–8342.
15. Aramini, J. M.; Mujeeb, A.; Germann, M. W. *Nucleic Acids Res.*, **1998**, *26*, 5644–5654.
16. Aramini, J. M.; Germann, M. W. *Biochemistry*, **1999**, *38*, 15448–15458.
17. Aramini, J. M.; Kalisch, B. W.; Pon, R. T.; van de Sande, J. H.; Germann, M. W. *Biochemistry*, **1996**, *35*, 9355–9365.
18. Aramini, J. M.; Mujeeb, A.; Ulyanov, N. B.; Germann, M.W. *J. Biomol. NMR*, **2000**, in press.
19. Torda, A. E.; Scheek, R. M.; van Gunsteren, W. F. *J. Biol. Mol.*, **1990**, *214*, 223–235.
20. Pearlman, D. A.; Kollman, P. A. *J. Biol. Mol.*, **1991**, *220*, 457–479.
21. Görler, A.; Ulyanov, N.B.; James, T.L. *J. Biomol. NMR*, **2000**, *16*, 147–164, and references therein.
22. van Wijk, J.; Huckriede, B. D.; Ippel, J. H; Altona, C. *Methods Enzymol.*, **1992**, *211*, 286–306.
23. Ulyanov, N. B.; Schmitz, U.; Kumar, A; James, T. L. *Biophys. J.*, **1995**, *68*, 13–24.

Request Permission or Order Reprints Instantly!